Sensitivity Studies of the Time-Dependent Angular Analysis to Untagged $\mathrm{B}_{\mathrm{S}}^{0} \to \mathrm{J}/\psi\phi$ Events

Note

Issue: 1
Revision: 0

Reference: LHCb-INT-2010-047
Created: August 2010
Last modified: October 4, 2010

Prepared by:
Géraldine Conti[a], Adlène Hicheur[a], Tatsuya Nakada[a], Frédéric Blanc[a]

[a]EPFL, Switzerland

LHCb-INT-2010-047
04/10/2010

Abstract

In this document, we present sensitivity studies to the $\mathrm{B_s^0}$ mixing phase $\phi_\mathrm{s}^{\mathrm{J}/\psi\phi}$ in the case of a fit to untagged $\mathrm{B_s^0} \to \mathrm{J/\psi\phi}$ events at the LHCb detector. As this decay leads to an admixture of CP-even and CP-odd components in the final state, an angular analysis is required to separate statistically the two CP eigenstates. Sensitivity results for the full three-angle and time-dependent analysis are given, for a Standard Model ($\phi_\mathrm{s}^{\mathrm{J}/\psi\phi} \sim 0$ rad) and a New Physics ($\phi_\mathrm{s}^{\mathrm{J}/\psi\phi} \sim 0.6$ rad) scenarios.

Contents

1 Introduction

Decays of $\mathrm{B_s^0}$ mesons to $\mathrm{J}/\psi\phi$ either directly or through $\mathrm{B_s^0}$ - $\overline{\mathrm{B}}_\mathrm{s}^0$ oscillations lead to the CP violating phase $\phi_\mathrm{s}^{\mathrm{J}/\psi\phi}$. In the Standard Model, this phase is predicted to be $\phi_\mathrm{s}^{\mathrm{J}/\psi\phi} \equiv -2\beta_s = -0.0360^{+0.0020}_{-0.0016}$ rad [1], with β_s the smallest angle of the unitary triangle of the CKM matrix relevant to $\mathrm{B_s^0}$. This phase is hence one of the CP observables with the smallest theoretical uncertainty. A precise measurement of $\phi_\mathrm{s}^{\mathrm{J}/\psi\phi}$ could therefore lead to an indirect discovery of New Physics, in case new particles would contribute to the $\mathrm{B_s^0}$ - $\overline{\mathrm{B}}_\mathrm{s}^0$ box diagram and hence modify the $\phi_\mathrm{s}^{\mathrm{J}/\psi\phi}$ value from its Standard Model expectation. This makes it a key measurement at LHCb. On the way to this measurement, an analysis without tagging the flavor of the $\mathrm{B_s^0}$ at production will be first performed. In this document, sensitivity studies for the parameters that can be determined at LHCb from the time-dependent angular analysis to untagged $\mathrm{B_s^0} \to \mathrm{J}/\psi\phi$ events are presented, considering both Standard Model and New Physics scenarios.

1.1 Differential $\mathrm{B_s^0} \to \mathrm{J}/\psi\phi$ Decay Rates

The differential decay rates for $\mathrm{B_s^0}$ and $\overline{\mathrm{B}}_\mathrm{s}^0$ are given in Equations 1 and 2 respectively. The time-dependent terms $h_k(t)(\bar{h}_k(t))$ are expressed in terms of the transverse amplitudes (Tables 1-2). Their full expressions can be found in [1]. The time-dependent terms are independent of the angular terms $f_k^{\mathrm{TR/HEL}}(\vec{\Omega}_{\mathrm{TR/HEL}})$. The $f_k^{\mathrm{TR}}(\vec{\Omega}_{\mathrm{TR}})$ angular functions for the transversity basis are defined in Table 1 and the $f_k^{\mathrm{HEL}}(\vec{\Omega}_{\mathrm{HEL}})$ functions for the helicity basis in Table 2.

$$\frac{\mathrm{d}^4\Gamma(\mathrm{B_s^0} \to \mathrm{J}/\psi\phi)}{\mathrm{d}t\ \mathrm{d}\vec{\Omega}_{\mathrm{TR/HEL}}} \propto \sum_{k=1}^{6} h_k(t) f_k^{\mathrm{TR/HEL}}(\vec{\Omega}_{\mathrm{TR/HEL}}) \tag{1}$$

$$\frac{\mathrm{d}^4\Gamma(\overline{\mathrm{B}}_\mathrm{s}^0 \to \mathrm{J}/\psi\phi)}{\mathrm{d}t\ \mathrm{d}\vec{\Omega}_{\mathrm{TR/HEL}}} \propto \sum_{k=1}^{6} \overline{h}_k(t) f_k^{\mathrm{TR/HEL}}(\vec{\Omega}_{\mathrm{TR/HEL}}) \tag{2}$$

k	$h_k(t)$	$\overline{h}_k(t)$	$f_k^{\mathrm{TR}}(\theta,\psi,\varphi)[\times 32\pi/9]$
1	$\lvert A_0(t)\rvert^2$	$\lvert \bar{A}_0(t)\rvert^2$	$2\cos^2\psi \cdot (1 - \sin^2\theta \cdot \cos^2\varphi)$
2	$\lvert A_{\lvert\rvert}(t)\rvert^2$	$\lvert \bar{A}_{\lvert\rvert}(t)\rvert^2$	$\sin^2\psi \cdot (1 - \sin^2\theta \cdot \sin^2\varphi)$
3	$\lvert A_\perp(t)\rvert^2$	$\lvert \bar{A}_\perp(t)\rvert^2$	$\sin^2\psi \cdot \sin^2\theta$
4	$\Im\{A_{\lvert\rvert}^*(t)A_\perp(t)\}$	$\Im\{\bar{A}_{\lvert\rvert}^*(t)\bar{A}_\perp(t)\}$	$-\sin^2\psi \cdot \sin 2\theta \cdot \sin\varphi$
5	$\Re\{A_0^*(t)A_{\lvert\rvert}(t)\}$	$\Re\{\bar{A}_0^*(t)\bar{A}_{\lvert\rvert}(t)\}$	$\frac{1}{\sqrt{2}}\sin 2\psi \cdot \sin^2\theta \cdot \sin 2\varphi$
6	$\Im\{A_0^*(t)A_\perp(t)\}$	$\Im\{\bar{A}_0^*(t)\bar{A}_\perp(t)\}$	$\frac{1}{\sqrt{2}}\sin 2\psi \cdot \sin 2\theta \cdot \cos\varphi$

Table 1 Angular functions $f_k^{\mathrm{TR}}(\theta,\psi,\varphi)$ in the transversity basis related to the time-dependent terms $h_k(t)$ expressed in the transversity basis.

k	$h_k(t)$	$\overline{h}_k(t)$	$f_k^{\mathrm{HEL}}(\theta_H,\psi,\chi)[\times 64\pi/9]$
1	$\lvert A_0(t)\rvert^2$	$\lvert \bar{A}_0(t)\rvert^2$	$4\cos^2\psi \cdot \sin^2\theta_H$
2	$\lvert A_{\lvert\rvert}(t)\rvert^2$	$\lvert \bar{A}_{\lvert\rvert}(t)\rvert^2$	$\sin^2\psi \cdot (1 + \cos^2\theta_\mathrm{H} - \sin^2\theta_\mathrm{H} \cdot \cos 2\chi)$
3	$\lvert A_\perp(t)\rvert^2$	$\lvert \bar{A}_\perp(t)\rvert^2$	$\sin^2\psi \cdot (1 + \cos^2\theta_\mathrm{H} + \sin^2\theta_\mathrm{H} \cdot \cos 2\chi)$
4	$\Im\{A_{\lvert\rvert}^*(t)A_\perp(t)\}$	$\Im\{\bar{A}_{\lvert\rvert}^*(t)\bar{A}_\perp(t)\}$	$2\sin^2\psi \cdot \sin^2\theta_\mathrm{H} \cdot \sin 2\chi$
5	$\Re\{A_0^*(t)A_{\lvert\rvert}(t)\}$	$\Re\{\bar{A}_0^*(t)\bar{A}_{\lvert\rvert}(t)\}$	$-\sqrt{2}\sin 2\psi \cdot \sin 2\theta_\mathrm{H} \cdot \cos\chi$
6	$\Im\{A_0^*(t)A_\perp(t)\}$	$\Im\{\bar{A}_0^*(t)\bar{A}_\perp(t)\}$	$\sqrt{2}\sin 2\psi \cdot \sin 2\theta_\mathrm{H} \cdot \sin\chi$

Table 2 Angular functions $f_k^{\mathrm{HEL}}(\theta_\mathrm{H},\psi,\chi)$ in the helicity basis related to the time-dependent terms $h_k(t)$ expressed in the transversity basis.

In the analysis to untagged $\mathrm{B_s^0} \to \mathrm{J}/\psi\phi$ events , the differential decay rates of the $\mathrm{B_s^0}$ and the $\overline{\mathrm{B}}_\mathrm{s}^0$ are equally added and weighted by a factor 0.5 to satisfy to the value of the total decay rate (Equation 3). As the angular functions, $f_k^{\mathrm{TR}}(\theta,\psi,\varphi)$ for the transversity basis or $f_k^{\mathrm{HEL}}(\theta_\mathrm{H},\psi,\chi)$ for the helicity basis, are the same for both $h_k(t)$ and $\overline{h}_k(t)$ (Tables 1-2), only the time-dependent terms get modified as $u_k(t) = 0.5 \cdot (h_k(t) + \overline{h}_k(t))$, using $|A_j(t)| = |\bar{A}_j(t)|$ with $j = \{0, ||, \perp\}$ from [1]:

$$\frac{\mathrm{d}^4\Gamma(\mathrm{B_s^0}/\overline{\mathrm{B}}_\mathrm{s}^0 \to J/\psi\phi)}{\mathrm{d}t\ \mathrm{d}\vec{\Omega}_{\mathrm{TR/HEL}}} = 0.5 \cdot \frac{\mathrm{d}^4\Gamma(\mathrm{B_s^0} \to \mathrm{J}/\psi\phi)}{\mathrm{d}t\ \mathrm{d}\vec{\Omega}_{\mathrm{TR/HEL}}} + 0.5 \cdot \frac{\mathrm{d}^4\Gamma(\overline{\mathrm{B}}_\mathrm{s}^0 \to \mathrm{J}/\psi\phi)}{\mathrm{d}t\ d\vec{\Omega}_{\mathrm{TR/HEL}}} \propto \sum_{k=1}^{6} u_k(t) f_k^{\mathrm{TR/HEL}}(\vec{\Omega}_{\mathrm{TR/HEL}}) \tag{3}$$

$$u_1(t) = \frac{1}{2}\cdot \quad \left(|A_0(t)|^2 + |\bar{A}_0(t)|^2\right) = \quad |A_0|^2 \mathrm{e}^{-\Gamma_\mathrm{s} t} \cdot \left[\cosh\left(\frac{\Delta\Gamma_\mathrm{s} t}{2}\right) - \cos\left(\phi_\mathrm{s}^{\mathrm{J}/\psi\phi}\right)\sinh\left(\frac{\Delta\Gamma_\mathrm{s} t}{2}\right)\right] \tag{4}$$

$$u_2(t) = \frac{1}{2}\cdot \quad \left(|A_\parallel(t)|^2 + |\bar{A}_\parallel(t)|^2\right) = \quad |A_\parallel|^2 \mathrm{e}^{-\Gamma_\mathrm{s} t} \cdot \left[\cosh\left(\frac{\Delta\Gamma_\mathrm{s} t}{2}\right) - \cos\left(\phi_\mathrm{s}^{\mathrm{J}/\psi\phi}\right)\sinh\left(\frac{\Delta\Gamma_\mathrm{s} t}{2}\right)\right] \tag{5}$$

$$u_3(t) = \frac{1}{2}\cdot \quad \left(|A_\perp(t)|^2 + |\bar{A}_\perp(t)|^2\right) = \quad |A_\perp|^2 \mathrm{e}^{-\Gamma_\mathrm{s} t} \cdot \left[\cosh\left(\frac{\Delta\Gamma_\mathrm{s} t}{2}\right) + \cos\left(\phi_\mathrm{s}^{\mathrm{J}/\psi\phi}\right)\sinh\left(\frac{\Delta\Gamma_\mathrm{s} t}{2}\right)\right] \tag{6}$$

$$u_4(t) = \frac{1}{2}\cdot\left(\Im\{A_\parallel^*(t)A_\perp(t)\} + \Im\{\bar{A}_\parallel^*(t)\bar{A}_\perp(t)\}\right) = |A_\parallel||A_\perp|\mathrm{e}^{-\Gamma_\mathrm{s} t} \cdot \left[- \sin\left(\phi_\mathrm{s}^{\mathrm{J}/\psi\phi}\right)\sinh\left(\frac{\Delta\Gamma_\mathrm{s} t}{2}\right)\right] \cdot \cos(\delta_\perp - \delta_\parallel) \tag{7}$$

$$u_5(t) = \frac{1}{2}\cdot \quad \left(\Re\{A_0^*(t)A_\parallel(t)\} + \Re\{\bar{A}_0^*(t)\bar{A}_\parallel(t)\}\right) = |A_0||A_\parallel|\mathrm{e}^{-\Gamma_\mathrm{s} t} \cdot \left[\cosh\left(\frac{\Delta\Gamma_\mathrm{s} t}{2}\right) - \cos\left(\phi_\mathrm{s}^{\mathrm{J}/\psi\phi}\right)\sinh\left(\frac{\Delta\Gamma_\mathrm{s} t}{2}\right)\right] \cdot \cos(\delta_\parallel) \tag{8}$$

$$u_6(t) = \frac{1}{2}\cdot \left(\Im\{A_0^*(t)A_\perp(t)\} + \Im\{\bar{A}_0^*(t)\bar{A}_\perp(t)\}\right) = |A_0||A_\perp|\mathrm{e}^{-\Gamma_\mathrm{s} t} \cdot \left[- \sin\left(\phi_\mathrm{s}^{\mathrm{J}/\psi\phi}\right)\sinh\left(\frac{\Delta\Gamma_\mathrm{s} t}{2}\right)\right] \cdot \cos(\delta_\perp) \tag{9}$$

All the terms containing the Δm_s parameter in the time-dependent quadratic and interfering amplitude terms of vanish, as they have opposite signs between terms for $\mathrm{B_s^0}$ and $\overline{\mathrm{B}}_\mathrm{s}^0$ mesons [1]. The resulting untagged analysis therefore counts seven free physical parameters:

- The width difference: $\Delta\Gamma_\mathrm{s} = \Gamma_\mathrm{L} - \Gamma_\mathrm{H}$
- The $\mathrm{B_s^0}$ meson lifetime τ_s or equivalently: $\Gamma_\mathrm{s} = 1/\tau_s$
- The fraction of CP-odd component at $t = 0\ s$: $|A_\perp|^2$
- The fraction of CP-even component at $t = 0\ s$ corresponding to $\ell = 0$: $|A_0|^2$
- The parallel CP conserving strong phase: $\delta_{||} = \arg(A_{||}A_0^*)$
- The perpendicular CP conserving strong phase: $\delta_\perp = \arg(A_\perp A_0^*)$
- The CP violating weak phase $\phi_\mathrm{s}^{\mathrm{J}/\psi\phi}$

2 The Fit Model

The fit model presented here is defined in [2] (version v2) as the latest available official model recommended by the LHCb β_s working group to be used for sensitivity studies to $\phi_\mathrm{s}^{\mathrm{J}/\psi\phi}$. It is therefore the one used in Section 5. The model comprises three parts, the proper time, the angular and the mass models, which are described in the following separately for each the signal, long-lived background and prompt background contributions.

2.1 The Model for Proper Time Distribution

Signal

The time-dependent terms $u_k(t)$ of Equations 4-9 of the untagged analysis are convoluted [a] with a proper time resolution function $PR_{\mathrm{S}}(t)$ describing the resolution of the LHCb spectrometer on the proper time measurement

$$u'_k(t) = u_k(t) \otimes PR_{\mathrm{S}}(t) \tag{10}$$

with the $PR_{\mathrm{S}}(t)$ resolution function being a triple Gaussian

$$PR_{\mathrm{S}}(t) = f_{(t,\mathrm{S},1)} \cdot \mathcal{G}(\mu_{(t,\mathrm{S},1)}, \sigma_{(t,\mathrm{S},1)}) + f_{(t,\mathrm{S},2)} \cdot \mathcal{G}(\mu_{(t,\mathrm{S},2)}, \sigma_{(t,\mathrm{S},2)}) + (1 - f_{(t,\mathrm{S},1)} - f_{(t,\mathrm{S},2)}) \cdot \mathcal{G}(\mu_{(t,\mathrm{S},3)}, \sigma_{(t,\mathrm{S},3)}) \tag{11}$$

Instead of using a triple Gaussian in the fit model, a single Gaussian with a mean proper time resolution $\langle \sigma_{(t,\mathrm{S})} \rangle$ is used, which is calculated as:

$$\langle \sigma_{(t,\mathrm{S})} \rangle = \sqrt{f_{(t,\mathrm{S},1)} \cdot \sigma^2_{(t,\mathrm{S},1)} + f_{(t,\mathrm{S},2)} \cdot \sigma^2_{(t,\mathrm{S},2)} + (1 - f_{(t,\mathrm{S},1)} - f_{(t,\mathrm{S},2)}) \cdot \sigma^2_{(t,\mathrm{S},3)}} \tag{12}$$

In Monte Carlo studies only, the proper time resolution can be obtained by fitting the $\mathrm{PR_S}(t)$ function to the residual distribution between the reconstructed and generated proper times of the L0-, HLT1-triggered and selected Monte Carlo $\mathrm{B_s^0} \to \mathrm{J}/\psi\phi$ signal events. This is not possible for real data. Instead, the proper time resolution will be estimated from a fit to the reconstructed proper time using an exponential function with an average lifetime τ_{eq} convoluted with a single Gaussian to model the resolution. τ_{eq} can be expressed as a function of the two states composing the $\mathrm{B_s^0}$ meson that evolve in time with τ_{L} and τ_{H} [1].

$$\begin{aligned} \tau_{\mathrm{eq}} = \frac{1}{\Gamma} \quad = \quad & \left((1 - \cos\left(\phi_{\mathrm{s}}^{\mathrm{J}/\psi\phi}\right)) \frac{|A_0|^2}{2} + (1 - \cos\left(\phi_{\mathrm{s}}^{\mathrm{J}/\psi\phi}\right)) \frac{|A_{||}|^2}{2} + (1 + \cos\left(\phi_{\mathrm{s}}^{\mathrm{J}/\psi\phi}\right)) \frac{|A_{\perp}|^2}{2} \right) \tau_{\mathrm{H}} + \\ & \left((1 + \cos\left(\phi_{\mathrm{s}}^{\mathrm{J}/\psi\phi}\right)) \frac{|A_0|^2}{2} + (1 + \cos\left(\phi_{\mathrm{s}}^{\mathrm{J}/\psi\phi}\right)) \frac{|A_{||}|^2}{2} + (1 - \cos\left(\phi_{\mathrm{s}}^{\mathrm{J}/\psi\phi}\right)) \frac{|A_{\perp}|^2}{2} \right) \tau_{\mathrm{L}} \end{aligned} \tag{13}$$

In the $\mathrm{B_s^0} \to \mathrm{J}/\psi\phi$ DC06 Monte Carlo event generation, $\tau_{\mathrm{L}} = 1.391$ ps and $\tau_{\mathrm{H}} = 1.538$ ps have been used, leading to $\tau_{\mathrm{eq}} = 1.415$ ps. From the fit of the true and reconstructed proper time distributions, this value has been found back within the errors [3]. An average resolution $\langle \sigma_{(t,\mathrm{S})} \rangle = 0.039$ ps is obtained, with similar results for the $\mathrm{B^0} \to \mathrm{J}/\psi\mathrm{K^{*0}}$ and $\mathrm{B^+} \to \mathrm{J}/\psi\mathrm{K^+}$ control channels and from a fit of the prompt component of the background [2].

The measurement of the proper time t is the result of a measurement of the distance between the primary and $\mathrm{B_s^0}$ decay vertices and $\mathrm{B_s^0}$ momentum. Its uncertainty is dominated by the former. The proper time resolution model can thus be improved by taking into account the vertex position uncertainties varying from event to event (dt), leading to a per-event proper time resolution model [4]. However, studies indicate that for a data statistics below 2 $\mathrm{fb^{-1}}$, using per event proper time uncertainties instead of a constant proper time error does not significantly improve the sensitivity to $\phi_{\mathrm{s}}^{\mathrm{J}/\psi\phi}$ [1]. Therefore, the constant proper time resolution $\langle \sigma_{(t,\mathrm{S})} \rangle = 0.039$ ps is used in the sensitivity studies of Section 5, together with the assumption of a flat proper time acceptance [2].

Long-Lived Background

In Monte Carlo studies, the proper time of the long-lived background is obtained by fitting with a fit function $P_{\mathrm{LL}}(t)$ the proper time distribution of events coming from the $\mathrm{B_{u,d,s}} \to \mathrm{J}/\psi\mathrm{X}$ inclusive sample, after removing the signal contribution [1]. $P_{\mathrm{LL}}(t)$ is a double exponential decay function convoluted with a single Gaussian function:

$$P_{\mathrm{LL}}(t) = \left(f_{(t,\mathrm{LL},1)} \cdot \mathrm{e}^{-\frac{t}{\tau_{(t,\mathrm{LL},1)}}} + (1 - f_{(t,\mathrm{LL},1)}) \cdot \mathrm{e}^{-\frac{t}{\tau_{(t,\mathrm{LL},2)}}} \right) \otimes \mathcal{G}(t, \sigma_{t,\mathrm{LL}}) \tag{14}$$

[a] The symbol $\otimes$ is used for the convolution.

Using DC06 events, the mean lifetimes are found to be $\tau_{(t,\mathrm{LL},1)} = 0.161$ ps and $\tau_{(t,\mathrm{LL},2)} = 1.114$ ps with a relative fraction $f_{(t,\mathrm{LL},1)} = 0.78$ and the width is found to be $\sigma_{(t,\mathrm{LL})} = 0.066$ ps [2] [b].

Prompt Background

In Monte Carlo studies, the proper time of the prompt background is obtained by fitting with a fit function $P_{\mathrm{Pr}}(t)$ the proper time distribution of events coming from the $\mathrm{J/\psi} \to \mu\mu$ inclusive sample, after removing the signal contribution [1]. $P_{\mathrm{Pr}}(t)$ is a single Gaussian:

$$P_{\mathrm{Pr}}(t) = \mathcal{G}(\mu_{(t,\mathrm{Pr})}, \sigma_{(t,\mathrm{Pr})}) \tag{15}$$

Using DC06 events, the width is found to be $\sigma_{(t,\mathrm{Pr})} = 0.044$ ps [2] [b].

2.2 The Model for Angular Distribution

Signal

The angular functions $f_k^{\mathrm{TR}}(\theta,\psi,\varphi)$ and $f_k^{\mathrm{HEL}}(\theta_{\mathrm{H}},\psi,\chi)$ for the decay final states of the signal are defined in Table 1 for the transversity basis and in Table 2 for the helicity basis. In principle, they must be convoluted with angular resolution functions $AR_{(S,\Omega_{\mathrm{TR/HEL,i}})}(f(\Omega_{\mathrm{TR/HEL,i}}))$, with $\Omega_{\mathrm{TR}} = \{\theta,\psi,\varphi\}$ for the transversity angles or $\Omega_{\mathrm{HEL}} = \{\theta_{\mathrm{H}},\psi,\chi\}$ for the helicity ones, to take into account the effect of the LHCb spectrometer on the angle measurements:

$$\begin{aligned} f_k^{'\mathrm{TR}}(\theta,\psi,\varphi) &= f_k^{\mathrm{TR}}(\theta,\psi,\varphi) \quad \otimes AR_{\mathrm{S},\theta}(\cos(\theta)) \quad \otimes AR_{\mathrm{S},\psi}(\cos(\psi)) \otimes AR_{\mathrm{S},\varphi}(\varphi) \\ f_k^{'\mathrm{HEL}}(\theta_{\mathrm{H}},\psi,\chi) &= f_k^{\mathrm{HEL}}(\theta_{\mathrm{H}},\psi,\chi) \otimes AR_{\mathrm{S},\theta_{\mathrm{H}}}(\cos(\theta_{\mathrm{H}})) \otimes AR_{\mathrm{S},\psi}(\cos(\psi)) \otimes AR_{\mathrm{S},\chi}(\chi) \end{aligned} \tag{16}$$

The angular resolutions have been estimated for the angles of the transversity basis to be $27\ \mathrm{mrad}$ for θ, $27\ \mathrm{mrad}$ for ϕ and $20\ \mathrm{mrad}$ for ψ from triple-Gaussian fits to the residual distribution between the reconstructed and the generated angles of L0-, HLT1-triggered and offline-selected DC06 signal $\mathrm{B_s^0} \to \mathrm{J/\psi\phi}$ events [1]. These angular distributions are not included in the model used for the sensitivity studies [2].

The angular acceptances for the signal are also neglected in the fit model [2]. However, a description of the angular acceptance is developed using MC09 Monte Carlo data in [5], where the importance of taking them eventually into account in the analysis on real data is highlighted.

Long-Lived and Prompt Background

Flat angular distribution models $A_{\mathrm{LL}}(\Omega_{\mathrm{TR/HEL}})$ and $A_{\mathrm{Pr}}(\Omega_{\mathrm{TR/HEL}})$ without angular acceptance descriptions are used in the fit model for the long-lived and prompt background components respectively [2]. However, some acceptance variations in the decay angles have been observed for the long-lived background, which are the result of the non-negligible fraction of partially reconstructed signal events. For the prompt component, no acceptance variations in the decay angles are observed, which is due to the fact that most of the events come from combinatorics [1].

2.3 The Model for Mass Distribution

Signal

The mass distribution for the signal is obtained by fitting the $\mu^+\mu^-\mathrm{K}^+\mathrm{K}^-$ invariant mass distribution of the L0-, HLT1-triggered and offline-selected $\mathrm{B_s^0} \to \mathrm{J/\psi\phi}$ events with a triple-Gaussian $M_{\mathrm{S}}(m)$:

$$M_{\mathrm{S}}(m) = f_{(m,\mathrm{S},1)} \cdot \mathcal{G}(\mu_{(m,\mathrm{S},1)}, \sigma_{(m,\mathrm{S},1)}) + f_{(m,\mathrm{S},2)} \cdot \mathcal{G}(\mu_{(m,S,2)}, \sigma_{(m,\mathrm{S},2)}) + (1 - f_{(m,\mathrm{S},1)} - f_{(m,\mathrm{S},2)}) \cdot \mathcal{G}(\mu_{(m,\mathrm{S},3)}, \sigma_{(m,\mathrm{S},3)}) \tag{17}$$

[b] The values quoted here are nearly identical to the parameters extracted from the fits to the distributions of Figures 14-15 of [1] (p.181). The small differences arise from the fact that the selection analyses kept evolving after the parameters were frozen for the fit studies.

The average mass resolution $\langle\sigma_{(m,\mathrm{S})}\rangle$ is calculated as:

$$\langle\sigma_{(m,\mathrm{S})}\rangle = \sqrt{f_{(m,\mathrm{S},1)} \cdot \sigma^2_{(m,\mathrm{S},1)} + f_{(m,\mathrm{S},2)} \cdot \sigma^2_{(m,\mathrm{S},2)} + (1 - f_{(m,\mathrm{S},1)} - f_{(m,\mathrm{S},2)}) \cdot \sigma^2_{(m,\mathrm{S},3)}} \tag{18}$$

For DC06 Monte Carlo data, the average mass resolution obtained is $\langle\sigma_{(m,S)}\rangle = 16.2\ \mathrm{MeV/c^2}$ [2].

Long-Lived Background

The mass distribution for the long-lived background is obtained by fitting the $\mu^+\mu^-\mathrm{K}^+\mathrm{K}^-$ invariant mass distribution of the $\mathrm{B_{u,d,s}} \to \mathrm{J}/\psi\mathrm{X}$ inclusive sample with an exponential function $M_{\mathrm{LL}}(m)$, after removing the signal contribution [1].

$$M_{\mathrm{LL}}(m) = \mathrm{e}^{-\alpha_{(m,\mathrm{LL})} \cdot m} \tag{19}$$

The slope is found to be $\alpha_{(m,\mathrm{LL})} = 0.001\ (\mathrm{MeV}/c^2)^{-1}$ [2] [b].

Prompt Background

The mass distribution for the prompt background is obtained by fitting the $\mu^+\mu^-\mathrm{K}^+\mathrm{K}^-$ invariant mass distribution of the $\mathrm{J}/\psi \to \mu\mu$ inclusive sample with an exponential function $M_{\mathrm{Pr}}(m)$, after removing the signal contribution [1].

$$M_{\mathrm{Pr}}(m) = \mathrm{e}^{-\alpha_{(m,\mathrm{Pr})} \cdot m} \tag{20}$$

The slope is found to be $\alpha_{(m,\mathrm{Pr})} = 0.0006\ (\mathrm{MeV}/c^2)^{-1}$ [2] [b].

2.4 The Full Fit Model

The *Probability Density Function (PDF)* for the proper time, angles and mass for the signal, $S(t, \Omega_{\mathrm{TR/HEL}}, m)$, can be factorized between that of Equation 3 (corrected for taking into account the convolution with the proper time resolution model leading to the $u'_k(t)$ terms of Equation 10) and that for the invariant mass distribution of Equation 17:

$$S(t, \Omega_{\mathrm{TR/HEL}}, m) = \left(\sum_{k=1}^{6} u'_k(t) f_k^{\mathrm{TR/HEL}}(\Omega_{\mathrm{TR/HEL}}) \right) \cdot M_{\mathrm{S}}(m) \tag{21}$$

The probability density function for the proper time, angles and mass for the long-lived background, $B_{LL}(t, \Omega_{\mathrm{TR/HEL}}, m)$, is given by

$$B_{\mathrm{LL}}(t, \Omega_{\mathrm{TR/HEL}}, m) = P_{\mathrm{LL}}(t) \cdot A_{\mathrm{LL}}(\Omega_{\mathrm{TR/HEL}}) \cdot M_{\mathrm{LL}}(m) \tag{22}$$

and for the prompt background $B_{\mathrm{Pr}}(t, \Omega_{\mathrm{TR/HEL}}, m)$ by

$$B_{\mathrm{Pr}}(t, \Omega_{\mathrm{TR/HEL}}, m) = P_{\mathrm{Pr}}(t) \cdot A_{\mathrm{Pr}}(\Omega_{\mathrm{TR/HEL}}) \cdot M_{\mathrm{Pr}}(m) \tag{23}$$

The total probability density function, $\mathcal{P}_{tot}$, for the proper time, angles and mass for the signal, long-lived background and prompt background is the sum of the three contributions weighted by the fractions of the signal $f_S = 0.30$ and of the long-lived background $f_{LL} = 0.15$ [2]:

$$\mathcal{P}_{\mathrm{tot}} = f_S \cdot S(t, \Omega_{\mathrm{TR/HEL}}, m) + f_{\mathrm{LL}} \cdot B_{\mathrm{LL}}(t, \Omega_{\mathrm{TR/HEL}}, m) + (1 - f_{\mathrm{S}} - f_{\mathrm{LL}}) \cdot B_{\mathrm{Pr}}(t, \Omega_{\mathrm{TR/HEL}}, m) \tag{24}$$

The fractions and detector parameters used in the fit model are summarized in Table 3.

DC06 MC Studies	Signal	Prompt Background	Long-Lived Background
Number of selected $\mathrm{B_s^0}$ events in a ± 50 MeV/c^2 signal mass window (2 fb^{-1} at $\sqrt{s}$ =14 TeV)	$117,000$	$210,600$ $(B/S = 1.8)$	$58,500$ $(B/S = 0.5)$
Proper Time Model	$S(t)$ No Acceptance Dependence	$P_{\mathrm{Pr}}(t) = \mathcal{G}(\mu, \sigma)$ with $\mu = 0$ ps, $\sigma = 0.044$ ps	$P_{\mathrm{LL}}(t) = [f \cdot \exp(-t/\tau_1) + (1-f) \cdot \exp(t/\tau_2)] \otimes \mathcal{G}(\mu, \sigma)$ with $f = 0.78$, $\tau_1 = 0.161$ ps, $\tau_2 = 1.114$ ps, $\mu = 0$ ps, $\sigma = 0.066$ ps
Angular Model	$S(\Omega_{\mathrm{TR/HEL}})$ No Resolution, No Acceptance Dependence	$A_{\mathrm{Pr}}(\Omega_{\mathrm{TR/HEL}})$ (flat) No Acceptance Dependence	$A_{\mathrm{LL}}(\Omega_{\mathrm{TR/HEL}})$ (flat) No Acceptance Dependence
Mass Model	$M_{\mathrm{S}}(m) = \mathcal{G}(\mu, \langle\sigma_{(m,S)}\rangle)$ with $\mu = 5.3664$ GeV/c^2, $\langle\sigma_{(m,\mathrm{S})}\rangle = 16.2$ MeV/c^2	$M_{\mathrm{Pr}}(m) = \exp(-\alpha \cdot m)$ with $\alpha = 0.0006$ (MeV/c^2)$^{-1}$	$M_{\mathrm{LL}}(m) = \exp(-\alpha \cdot m)$ with $\alpha = 0.001$ (MeV/c^2)$^{-1}$

Table 3 Parameters used for the toy Monte Carlo sensitivity studies for the fit to untagged $\mathrm{B_s^0} \to \mathrm{J/\psi\phi}$ events.

3 Fit Procedure

The physics parameters $\lambda_{\rm phys} = \left\{|A_0|^2, |A_\perp|^2, \Delta\Gamma_{\rm s}, \Gamma_{\rm s}, \delta_{||}, \delta_\perp, \phi_{\rm s}^{\rm J/\psi\phi}\right\}$ are determined by an unbinned log likelihood method from the measured event physics attributes $X_e = \{t, \Omega_{\rm TR/HEL}, m\}$. The detector parameters $\lambda_{\rm det} = \{\sigma_m, \sigma_t\}$ [c] and the background properties are also taken into account in the probability density function $\mathcal{P}_{\rm tot}$. Grouping together the physics and detector parameters as $\lambda = \{\lambda_{\rm phys} + \lambda_{\rm det}\}$, the likelihood function $\mathcal{L}$ of N events is expressed as:

$$\mathcal{L} = \prod_e^N \mathcal{P}_{\rm tot}(X_e; \lambda) \tag{25}$$

Instead of maximizing the likelihood product $\mathcal{L}$ of Equation 25, the negative logarithmic likelihood $\mathcal{L}'$ is minimized. The numerical instabilities arising from a large number of multiplications to be performed are hence prevented. $\mathcal{L}'$ is given by:

$$\mathcal{L}' = -\sum_e^N \ln(\mathcal{P}_{\rm tot}(X_e; \lambda)) \tag{26}$$

Two independent fitters are used to perform the unbinned likelihood fit to the untagged $\mathrm{B_s^0} \to \mathrm{J/\psi\phi}$ events for the sensitivity studies of Section 5. The first fitter, called *P2VV fitter*, is implemented in python language [8] and uses pre-defined functions available in the RooFit package [9]. The minimization uses by default the MIGRAD algorithm of the MINUIT package [10], which returns symmetric errors. The second fitter, called *Heidelberg fitter*, is implemented using the C++ coding language [11]. The minimization is also performed with the MIGRAD algorithm.

Once the fit is achieved, both fitters provide displays showing the projections of the PDF on the basis angles and proper time, together with the CP-even and CP-odd contributions determined from the output fit values. An illustration of such displays is shown for the transversity angles in Figure 1, where only the signal contribution has been used in the generation and fit.

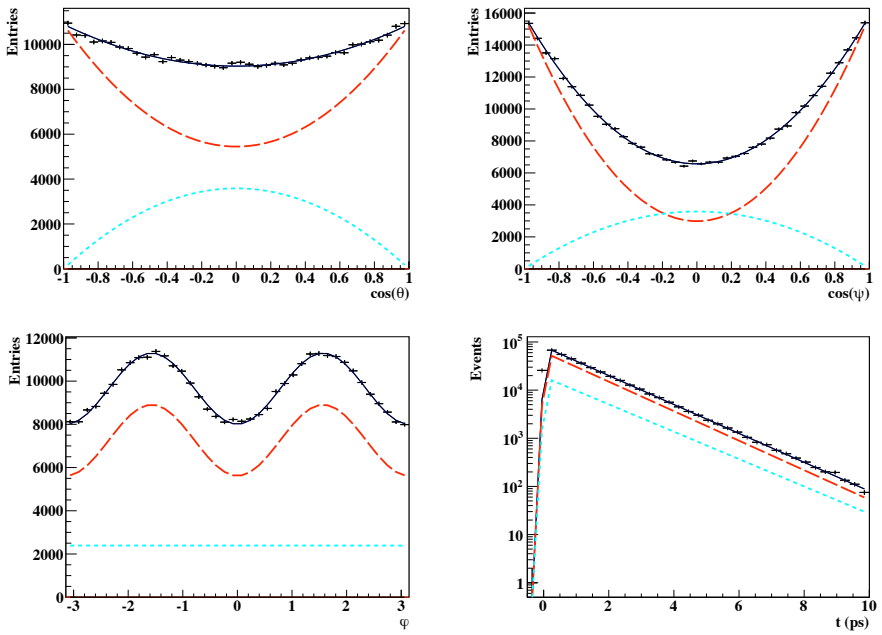

Figure 1 Angular and proper time distributions of the signal toy Monte Carlo data (black histogram), with the CP-even (red long-dashed line) and CP-odd (cyan short-dashed) components determined from the output fit values.

[c] The proper time and angular acceptances should be included in the detector parameters.

4 Latest Results from the Tevatron about $\phi_\mathrm{s}^{\mathrm{J}/\psi\phi}$

The D⊘ and CDF experiments at Fermilab are working on the time-dependent angular analysis to tagged $\mathrm{B_s^0} \to \mathrm{J}/\psi(\mu^+\mu^-)\phi(\mathrm{K^+K^-})$ events. The results presented at the Rencontres de Moriond in March 2010 [12] were based on $\sim$ 3000 and $\sim$ 2000 $\mathrm{B_s^0}$ signal events for CDF and D⊘ experiments respectively, corresponding to a luminosity of $2.8\ \mathrm{fb}^{-1}$ each. The results obtained for $\Delta\Gamma_\mathrm{s}$, τ_s and $\phi_\mathrm{s}^{\mathrm{J}/\psi\phi}$ are summarized in Table 4. The Δm_s parameter was constrained to $17.77 \pm 0.12\ \mathrm{ps}^{-1}$.

To estimate the deviation of the result from the Standard Model expectation, the *p-value* is calculated. It represents the chance of rejecting the SM hypothesis when it is true. The lower the p-value, the less likely the result is if the SM hypothesis is true, and consequently the more significant the result is. The combination of the CDF and D⊘ results of Table 4 has a p-value of 3.4% [13].

Parameter	D⊘ Experiment	CDF Experiment
$\Delta\Gamma_\mathrm{s}\ [\mathrm{ps}^{-1}]$	0.19 ± 0.07	0.02 ± 0.05
$\tau_\mathrm{s}\ [\mathrm{ps}]$	1.52 ± 0.06	1.53 ± 0.04
$\phi_\mathrm{s}^{\mathrm{J}/\psi\phi}\ [\mathrm{rad}]$	$-0.57^{+0.25}_{-0.30}$	$[-0.56, -2.58]\ (68\%)$

Table 4 $\Delta\Gamma_\mathrm{s}$, τ_s and $\phi_\mathrm{s}^{\mathrm{J}/\psi\phi}$ results from the CDF and D⊘ collaborations presented at the Rencontres de Moriond in March 2010 [12].

Since then, the CDF experiment has updated its result on $\phi_\mathrm{s}^{\mathrm{J}/\psi\phi}$ using $5.2\ \mathrm{fb}^{-1}$ of data [14]. The two-dimensional profile likelihood and the 68% and the 95% CL contours are shown in Figure 2 (left). The p-value is 44%, which means that the new result is in better agreement with the Standard Model than the previous ones (Table 4). The two solutions arising from the two-fold ambiguity explained in [1] are still equally probable and it is not yet possible to choose one over the other. From the β_s scan of Figure 2 (right), the following solutions are obtained for two different confidence levels, with a p-value of 31%:

- $\beta_s \in [0.02, 0.52] \cup [1.08, 1.55]$ at 68% CL
- $\beta_s \in [-0.13, 0.68] \cup [0.89, \pi/2] \cup [-\pi/2, -1.44]$ at 95% CL

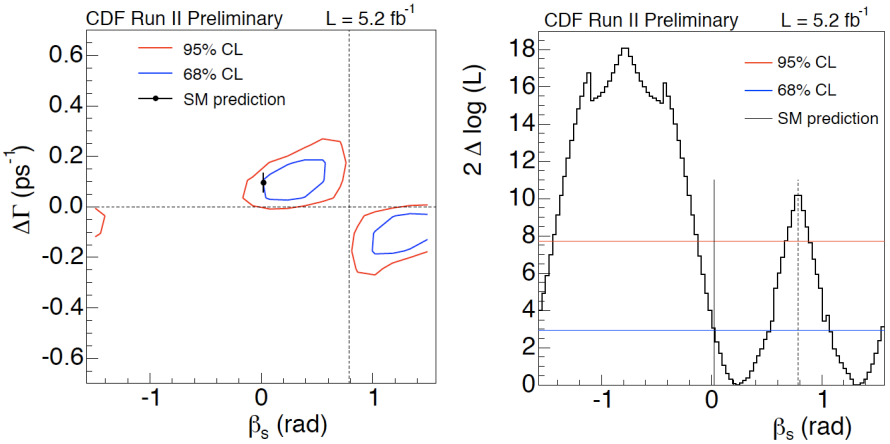

Figure 2 Updated result on β_s from CDF [14]: two-dimensional profile likelihood (left) and β_s scan (right).

Fixing β_s to zero, the $\mathrm{B_s^0}$ lifetime τ_s and the amplitudes $|\mathrm{A}_{||}|^2$ and $|\mathrm{A}_0|^2$ have been measured by CDF in the tagged analysis. Constraints are given on $\Delta\Gamma_\mathrm{s}$ and the strong phase $\delta_\perp$ (Table 5) [14] [d].

[d] The $\delta_{||}$ strong phase is floating in the fit. However, pull studies have shown non Gaussian behavior for this parameter, explaining why no best fit value is quoted for it. The Δm_s parameter is constrained within its error to its measured value in [?] using Gaussian constraints (see Subsection 5.2).

Parameter	Value	σ(stat)	σ(syst)
τ_{s} [ps]	1.53	± 0.025	± 0.012
$\Delta\Gamma_{\mathrm{s}}$ [ps^{-1}]	0.075	± 0.035	± 0.010
$\lvert \mathrm{A}_{\lvert\lvert} \rvert^2$	0.231	± 0.014	± 0.015
$\lvert \mathrm{A}_0 \rvert^2$	0.524	± 0.013	± 0.015
$\delta_\perp$ [rad]	2.95	± 0.640	± 0.070

Table 5 Latest results (June 2010) from the CDF experiment assuming $\beta_s = 0$ [14].

5 Time-Dependent Angular Analysis to Untagged $\mathrm{B_s^0} \to \mathrm{J/\psi\phi}$ Events

Compared to the time-dependent angular analysis to tagged $\mathrm{B_s^0} \to \mathrm{J/\psi\phi}$ events that will eventually bring the most precise measurement of $\phi_{\mathrm{s}}^{\mathrm{J/\psi\phi}}$, the fit to untagged $\mathrm{B_s^0} \to \mathrm{J/\psi\phi}$ events has the advantage of being independent of the understanding of the tagging. It is also less demanding regarding the proper time resolution, as it does not need to resolve the fast $\mathrm{B_s^0}$ - $\overline{\mathrm{B}}_{\mathrm{s}}^0$ oscillations. Indeed, the Δm_{s} parameter characterizing the frequency of the $\mathrm{B_s^0}$ - $\overline{\mathrm{B}}_{\mathrm{s}}^0$ mixing vanish in the untagged analysis (Equations 4-9). The fit to untagged $\mathrm{B_s^0} \to \mathrm{J/\psi\phi}$ events is therefore one of the first steps that will be performed with real data towards $\phi_{\mathrm{s}}^{\mathrm{J/\psi\phi}}$.

The time-dependent angular analysis to untagged $\mathrm{B_s^0} \to \mathrm{J/\psi\phi}$ events is a complicated procedure, including a simultaneous fit to several distributions, each depending on a number of unknown parameters. To estimate the measurement uncertainty, a *Toy Monte Carlo* technique is used. A simplified model of the measurement is build and a large number of identical jobs is performed, each with a different random number seed.

In the following studies, only the jobs for which the fit has converged are taken into account. For each physics parameter with input value x_{input}, the distributions of the returned best fit value, x_{fit}, the estimated error obtained from the covariance matrix of the fit, σ_x and the pull, Δx, defined in Equation 27 are plotted.

$$\Delta x = \frac{x_{\mathrm{fit}} - x_{\mathrm{input}}}{\sigma_x} \tag{27}$$

The sensitivity to the parameter x is defined as the width of the Gaussian fitted to the distribution of the returned values x_{fit}, which is checked to be consistent with the average of the fitted σ_x distribution. The pull distributions are examined to determine whether there are biases in the parameter determination. They are fitted with a Gaussian function. If the fit is not biased, the pull distribution should be centered to zero with a unit width.

The two P2VV [8] and Heidelberg [11] fitters explained in Section 3 are used in the sensitivity studies to cross-check the results [e]. Whenever possible, different scenarios are studied for the integrated luminosity per nominal year of data taking at $\sqrt{s} = 14$ TeV: 2 fb^{-1}, 0.2 fb^{-1} and 0.1 fb^{-1}. The numbers of generated $\mathrm{B_s^0} \to \mathrm{J/\psi\phi}$ events for the three statistical scenarios are obtained from Table 3 by scaling the integrated luminosity. They are given in Table 6.

Input from Simulation	Value
Background/Signal Ratio	
B_{prompt}/S	1.8
$B_{\mathrm{long-lived}}/S$	0.5
Total Event Number (S+B) ($\sqrt{s} = 14$ TeV)	
2.0 fb^{-1}	386,100
0.2 fb^{-1}	38,600
0.1 fb^{-1}	19,305

Table 6 Input from simulation used in the generation of standalone simplified Monte Carlo data and defined in [2] (version v2). The numbers correspond to a signal mass window of ± 50 MeV/c^2.

[e] The event generation is performed by each fitter separately.

The input values of the seven physics parameters used in the fit to untagged $\mathrm{B_s^0} \to \mathrm{J/\psi\phi}$ events are summarized in Table 7 [2]. These are based on constraints existing on Γ_s and $\Delta\Gamma_\mathrm{s}$. The input values of the other physics parameters rely on measurements performed in the $\mathrm{B^0} \to \mathrm{J/\psi K^{*0}}$ channel, except for the Standard Model $\phi_\mathrm{s}^{\mathrm{J}/\psi\phi}$ input value coming from an early 2008 estimate. The New Physics value for $\phi_\mathrm{s}^{\mathrm{J}/\psi\phi}$ is based on the latest result quoted by the D$\oslash$ experiment given in Table 4 [f].

Parameter	Value	Units	Source
Γ_s	0.680	ps^{-1}	[15]
$\Delta\Gamma_\mathrm{s}$	0.049	ps^{-1}	[15]
$\delta_{\|\|}$	-2.93	rad	[16]
$\|A_0\|^2$	0.556	-	[16]
$\|A_\perp\|^2$	0.233	-	[16]
$\delta_\perp$	2.91	rad	[16]
$\phi_\mathrm{s}^{\mathrm{J}/\psi\phi}(\mathrm{SM})$	-0.0368	rad	[19]
$\phi_\mathrm{s}^{\mathrm{J}/\psi\phi}(\mathrm{NP})$	-0.6000	rad	Table 4

Table 7 Physics parameters input values used in the fit to untagged $\mathrm{B_s^0} \to \mathrm{J/\psi\phi}$ events [2] (version v2). The δ_0 is set to zero by an allowed convention choice. The $|A_{\|\|}|^2$ parameter equals $|A_{\|\|}|^2 = 1 - |A_0|^2 - |A_\perp|^2 = 0.211$ [16].

The detector parameters are kept fixed in the following studies [g].

5.1 Standard Model Assumption

The $|A_0|^2$, $|A_\perp|^2$ and Γ_s parameters have recently been measured by the CDF experiment, as quoted in Table 5. Until now, the $\Delta\Gamma_\mathrm{s}$ and $\delta_{||}$ are only constrained by the measurements. The statistical uncertainties associated to the $|A_0|^2$, $|A_\perp|^2$ and Γ_s CDF measurements can be lowered significantly at LHCb and the $\Delta\Gamma_\mathrm{s}$ parameter can be measured assuming the Standard Model prediction for $\phi_\mathrm{s}^{\mathrm{J}/\psi\phi}$.

To perform the measurements, the $\phi_\mathrm{s}^{\mathrm{J}/\psi\phi}$ value is set to zero in the fit model to untagged $\mathrm{B_s^0} \to \mathrm{J/\psi\phi}$. As a consequence, the terms containing the $\delta_\perp$ strong phase in Equations 7 and 9 cancel. There is still an access to the strong phase $\delta_{||}$ through Equation 8.

From 300 Toy Monte Carlo jobs, it is observed that all the parameter input values are well retrieved and the errors calculated correctly, except for $\delta_{||}$. Indeed, in the distribution of the fitted $\delta_{||}$ values, several values are found to be equal to $-\pi$, as shown in Figure 3 (top). According to the MINUIT package returned message, the values at $-\pi$ result from successful minimizations.

To understand the origin of the fit output values at $-\pi$, a new parameterization, $a = \cos(\delta_{||})$, is introduced in the fit model. The jobs are redone using the same seeds than used previously. The distribution of the fitted $\cos(\delta_{||})$ values is shown in Figure 3 (middle), which is Gaussian-distributed. Some values are found to be smaller than -1, which correspond to unphysical regions probed during the minimization process. The possibility of having cosine values smaller than -1 is explained by the fact that the fit is not constrained anymore by the bounds imposed by the cosine function itself. Looking at the correlations between the $\delta_{||}$ output values at $-\pi$ and the values of $\cos(\delta_{||})$ belonging to unphysical regions (Figure 3, bottom), a full correlation is observed.

To estimate the parameter sensitivities, the jobs corresponding to output fit values $\delta_{||} = -\pi$ can therefore be considered as failed fits and removed. However, the errors on the remaining $\delta_{||}$ output fit values are not calculated properly, resulting in an asymmetric pull distribution. Hence, sensitivity results are given using the $a = \cos(\delta_{||})$ parameter instead, for which the error are correctly calculated. Three statistical scenarios are studied: $2\ \mathrm{fb}^{-1}$, $0.2\ \mathrm{fb}^{-1}$ and $0.1\ \mathrm{fb}^{-1}$ of data. The results are given in the upper parts of Tables 8, 9 and 10 respectively. In each case, 300 Toy Monte Carlo jobs are performed.

The sensitivities to the $|A_0|^2$, $|A_\perp|^2$, Γ_s and $\Delta\Gamma_\mathrm{s}$ parameters are found to be ± 0.003, ± 0.004, ± 0.003 ps^{-1} and ± 0.009 ps^{-1} respectively for the $2\ \mathrm{fb}^{-1}$ scenario [h]. The sensitivity to $\cos(\delta_{||})$ is ± 0.015 rad.

[f] This value is illustrative. It would need some re-tuning given the latest CDF result (Figure 2).
[g] The average value of the signal mass distribution, $m_{\mathrm{B_s^0}}$, is also fixed in the fit.
[h] Similar sensitivities are obtained when fixing the strong and weak phases (Appendix 8.1).

For the lower statistics cases, 0.2 fb^{-1} and 0.1 fb^{-1}, the sensitivities scale as $\sqrt{N}$, with N the number of $\mathrm{B_s^0} \to \mathrm{J}/\psi\phi$ events. With only 0.1 fb^{-1} of untagged data at $\sqrt{s} = 14$ TeV, the statistical uncertainties are of the same order of magnitude as the latest CDF results summarized in Table 5 obtained with a fit to tagged $\mathrm{B_s^0} \to \mathrm{J}/\psi\phi$ events. Moreover, the sensitivities quoted for $|A_0|^2$, $|A_\perp|^2$, Γ_s and $\Delta\Gamma_\mathrm{s}$ at 2 fb^{-1} are of the same order than the ones obtained from the tagged fit at LHCb [1].

The parameterization of the angular acceptance variations of [5], not used by default in the fit model, is added to check its impact on the sensitivity results. The results given in the lower part of Tables 8-10 show no differences with the sensitivity values obtained without angular acceptance description.

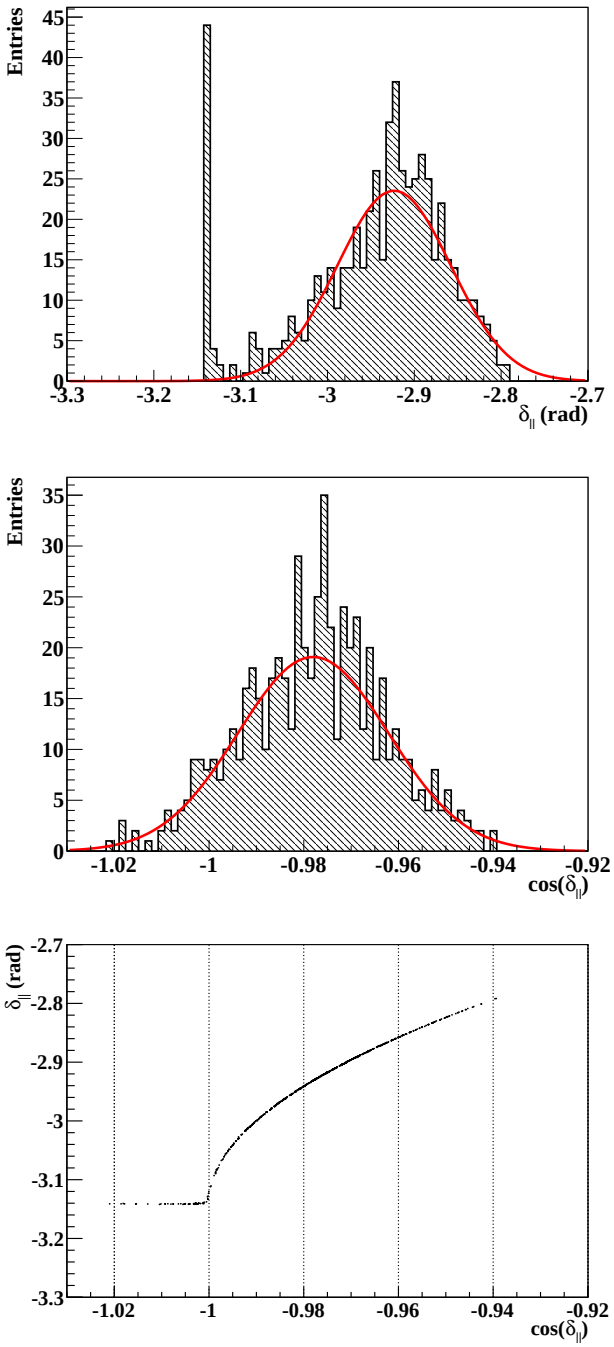

Figure 3 $\delta_{||}$ (top) and $a = \cos(\delta_{||})$ (middle) output fit value distributions obtained for the 2 fb^{-1} statistical scenario. The output fit values $\delta_{||} = -\pi$ (top) are fully correlated (bottom) with the values belonging to the unphysical region $\cos(\delta_{||}) < -1$ (middle).

Parameters	Value and Sensitivity	Pull Mean	Pull Width
$\lvert A_0\rvert^2$	0.556 ± 0.003	-0.03 ± 0.06	1.03 ± 0.04
$\lvert A_\perp\rvert^2$	0.233 ± 0.004	$+0.04 \pm 0.06$	1.00 ± 0.04
Γ_s $[\mathrm{ps}^{-1}]$	0.680 ± 0.003	-0.05 ± 0.06	1.04 ± 0.04
$\Delta\Gamma_\mathrm{s}$ $[\mathrm{ps}^{-1}]$	0.049 ± 0.009	-0.02 ± 0.06	0.96 ± 0.04
a	-0.978 ± 0.015	-0.03 ± 0.06	0.99 ± 0.04
Effect of Angular Acceptances (P2VV Fitter)			
$\lvert A_0\rvert^2$	0.556 ± 0.003	-0.08 ± 0.06	1.04 ± 0.04
$\lvert A_\perp\rvert^2$	0.233 ± 0.004	$+0.11 \pm 0.06$	1.05 ± 0.04
Γ_s $[\mathrm{ps}^{-1}]$	0.680 ± 0.003	-0.03 ± 0.06	1.04 ± 0.04
$\Delta\Gamma_\mathrm{s}$ $[\mathrm{ps}^{-1}]$	0.049 ± 0.008	$+0.02 \pm 0.06$	1.00 ± 0.04
a	-0.981 ± 0.015	-0.14 ± 0.06	1.01 ± 0.04

Table 8 Sensitivities and pull distribution parameters obtained for 2 fb^{-1} (Standard Model assumption).

Parameters	Value and Sensitivity	Pull Mean	Pull Width
Result With P2VV Fitter			
$\lvert A_0\rvert^2$	0.556 ± 0.009	-0.04 ± 0.06	1.05 ± 0.04
$\lvert A_\perp\rvert^2$	0.234 ± 0.012	$+0.05 \pm 0.06$	1.03 ± 0.04
Γ_s $[\mathrm{ps}^{-1}]$	0.680 ± 0.009	-0.03 ± 0.06	0.97 ± 0.04
$\Delta\Gamma_\mathrm{s}$ $[\mathrm{ps}^{-1}]$	0.048 ± 0.025	-0.03 ± 0.06	1.00 ± 0.04
a	-0.984 ± 0.048	-0.10 ± 0.06	1.00 ± 0.04
Effect of Angular Acceptances (P2VV Fitter)			
$\lvert A_0\rvert^2$	0.555 ± 0.008	-0.09 ± 0.06	1.05 ± 0.04
$\lvert A_\perp\rvert^2$	0.235 ± 0.012	$+0.15 \pm 0.06$	1.02 ± 0.04
Γ_s $[\mathrm{ps}^{-1}]$	0.680 ± 0.009	-0.01 ± 0.06	0.99 ± 0.04
$\Delta\Gamma_\mathrm{s}$ $[\mathrm{ps}^{-1}]$	0.046 ± 0.026	-0.09 ± 0.06	1.03 ± 0.04
a	-0.987 ± 0.048	-0.15 ± 0.06	1.03 ± 0.04

Table 9 Sensitivities and pull distribution parameters obtained for 0.2 fb^{-1} (Standard Model assumption).

Parameters	Value and Sensitivity	Pull Mean	Pull Width
Result With P2VV Fitter			
$\lvert A_0\rvert^2$	0.555 ± 0.012	-0.06 ± 0.06	1.10 ± 0.04
$\lvert A_\perp\rvert^2$	0.233 ± 0.017	$+0.01 \pm 0.06$	1.08 ± 0.04
Γ_s $[\mathrm{ps}^{-1}]$	0.681 ± 0.012	$+0.01 \pm 0.06$	1.00 ± 0.04
$\Delta\Gamma_\mathrm{s}$ $[\mathrm{ps}^{-1}]$	0.049 ± 0.037	$+0.03 \pm 0.06$	1.00 ± 0.04
a	-0.978 ± 0.070	$+0.05 \pm 0.06$	1.02 ± 0.04
Effect of Angular Acceptances (P2VV Fitter)			
$\lvert A_0\rvert^2$	0.556 ± 0.011	-0.03 ± 0.06	0.97 ± 0.04
$\lvert A_\perp\rvert^2$	0.234 ± 0.016	$+0.05 \pm 0.06$	0.94 ± 0.04
Γ_s $[\mathrm{ps}^{-1}]$	0.681 ± 0.012	$+0.00 \pm 0.06$	0.99 ± 0.04
$\Delta\Gamma_\mathrm{s}$ $[\mathrm{ps}^{-1}]$	0.046 ± 0.036	-0.04 ± 0.06	1.04 ± 0.04
a	-0.988 ± 0.068	-0.10 ± 0.06	1.00 ± 0.04

Table 10 Sensitivities and pull distribution parameters obtained for 0.1 fb^{-1} (Standard Model assumption).

It should be noted that when the $\delta_{||}$ input value is further away from $-\pi$, $\delta_{||} = -2.78$ rad for example, no output fit value at $-\pi$ is observed in the distribution, as shown in Figure 4 for 2 fb^{-1} of data.

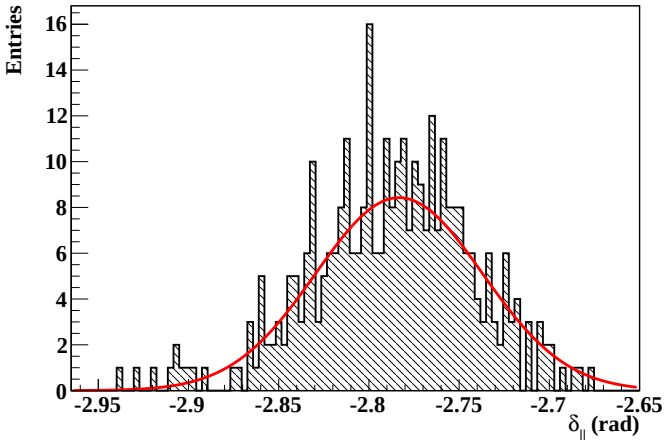

Figure 4 $\delta_{||}$ output fit value distribution using an input value $\delta_{||} = -2.78$ rad.

The associated sensitivity values and pull distribution parameters are given in Table 11. The sensitivity to $\delta_{||}$ is ± 0.046 rad.

Parameters	Value and Sensitivity	Pull Mean	Pull Width
$\lvert A_0\rvert^2$	0.556 ± 0.003	-0.03 ± 0.06	0.99 ± 0.04
$\lvert A_\perp\rvert^2$	0.233 ± 0.004	$+0.10 \pm 0.06$	1.04 ± 0.04
Γ_s [ps^{-1}]	0.680 ± 0.003	-0.02 ± 0.06	1.01 ± 0.04
$\Delta\Gamma_\mathrm{s}$ [ps^{-1}]	0.048 ± 0.008	-0.08 ± 0.06	0.99 ± 0.04
$\delta_{\lvert\rvert}$ [rad]	-2.783 ± 0.046	-0.07 ± 0.06	1.00 ± 0.04

Table 11 Sensitivities and pull distribution parameters for 2 fb^{-1} of Toy Monte Carlo data using $\delta_{||}$=-2.78 rad as input value (Standard Model assumption).

5.2 New Physics Scenario

In the Standard Model scenario, the sensitivity to $\phi_{\mathrm{s}}^{\mathrm{J}/\psi\phi}$ arises from the $\sin(\phi_{\mathrm{s}}^{\mathrm{J}/\psi\phi})$ terms, the $\cos(\phi_{\mathrm{s}}^{\mathrm{J}/\psi\phi})$ terms being almost insensitive due to the very small $\phi_{\mathrm{s}}^{\mathrm{J}/\psi\phi}$ expectation value. Luckily, $\sin(\phi_{\mathrm{s}}^{\mathrm{J}/\psi\phi})$ terms remain in two terms entering in the untagged formula (Equations 7, 9). However, they also depend on the strong phases $\delta_{||}$ and $\delta_{\perp}$ that have to be determined simultaneously in the fit. In the New Physics scenario, where the $\phi_{\mathrm{s}}^{\mathrm{J}/\psi\phi}$ value is set at 0.6 (Table 7), it is possible that the sensitivity is enhanced by the $\cos(\phi_{\mathrm{s}}^{\mathrm{J}/\psi\phi})$ terms.

If all the physics parameters are let free in the fit, the strong and weak phases cannot be measured [i]. Indeed, the $\delta_{\perp}$ input value, $\delta_{\perp} = 2.91$ rad, cannot be retrieved from the $\delta_{\perp}$ output fit value distribution shown in Figure 5 (left) for 2 fb^{-1} of Toy Monte Carlo data [j]. The $\delta_{||}$ output fit value distribution is similar to the one of Figure 3 (top), where several $\delta_{||}$ values are found to be $-\pi$ for an input value $\delta_{||} = -2.93$ rad. The $\phi_{\mathrm{s}}^{\mathrm{J}/\psi\phi}$ output fit value distribution is shown in Figure 5 (right), where the input value $\phi_{\mathrm{s}}^{\mathrm{J}/\psi\phi} = -0.6$ cannot be retrieved either. Therefore, in order to measure $\phi_{\mathrm{s}}^{\mathrm{J}/\psi\phi}$ with a fit to untagged $\mathrm{B_s^0} \to \mathrm{J}/\psi\phi$ events, the strong phases cannot be let free in the fit.

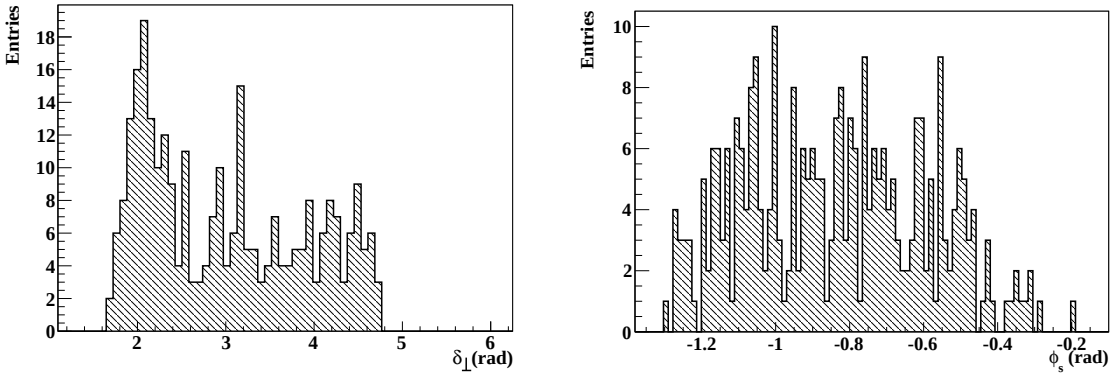

Figure 5 $\delta_{\perp}$ (left) and $\phi_{\mathrm{s}}^{\mathrm{J}/\psi\phi}$ (right) output fit value distributions obtained for 2 fb^{-1} of Toy Monte Carlo data, with all the physics parameters free in the fit. The input values of 2.91 rad for $\delta_{\perp}$ and -0.6 rad for $\phi_{\mathrm{s}}^{\mathrm{J}/\psi\phi}$ cannot be retrieved from the distributions.

The $\delta_{||}$ and $\delta_{\perp}$ strong phases have been measured by the Babar experiment in the $\mathrm{B^0} \to \mathrm{J}/\psi\mathrm{K}^{*0}$ channel to be $\delta_{||} = -2.93 \pm 0.08\,(\mathrm{stat}) \pm 0.04\,(\mathrm{syst})$ and $\delta_{\perp} = 2.91 \pm 0.05\,(\mathrm{stat}) \pm 0.03\,(\mathrm{syst})$ [16]. Under flavor symmetry, it is reasonable to assume that they are similar for the $\mathrm{B_s^0} \to \mathrm{J}/\psi\phi$ channel. They are indeed expected to be equal within a similar precision of a few percent of π (or $\sim 10^{\circ}$) [17]. Therefore, the strong phases δ_i $(i = \{||, \perp\})$ are constrained during the fit procedure using Gaussian error distributions to the values $\delta_{\mathrm{meas},i}$ measured by Babar, which are called *Gaussian constraints* [k].

The negative logarithmic likelihood of Equation 26 is modified as:

$$\mathcal{L}'' = -\sum_{e}^{N} \ln(\mathcal{P}_{\mathrm{tot}}(X_e;\lambda)) + \sum_{i} \frac{(\delta_i - \delta_{\mathrm{meas},i})^2}{2\sigma^2_{\mathrm{meas},i}} \tag{28}$$

where $\sigma_{\mathrm{meas},i}$ are the measurement uncertainties.

The sensitivity and pull distribution fit parameters are given in Table 12 for 1000 Toy Monte Carlo jobs at 2 fb^{-1} using external Gaussian constraints on both $\delta_{||}$ and $\delta_{\perp}$. The σ_{meas} is set at 0.18 rad, which is larger than the uncertainty on the $\delta_{||}$ and $\delta_{\perp}$ measurements, reducing the strength of the constraints in the fit. The distributions of the $\delta_{||}$, $\delta_{\perp}$ and $\phi_{\mathrm{s}}^{\mathrm{J}/\psi\phi}$ output fit value are shown in Figure 6.

[i] Small biases are also observed for Γ_{s} and $\Delta\Gamma_{\mathrm{s}}$.
[j] This is not the case for the tagged fit, where the $\delta_{\perp}$ input value is retrieved without any problem [1].
[k] This method has been used by the D$\oslash$ collaboration in the analysis to tagged $\mathrm{B_s^0} \to \mathrm{J}/\psi\phi$ events [18].

Parameters	Value and Sensitivity	Pull Mean	Pull Width
$\lvert A_0\rvert^2$	$+0.556 \pm 0.003$	-0.03 ± 0.03	1.03 ± 0.02
$\lvert A_\perp\rvert^2$	$+0.233 \pm 0.004$	$+0.01 \pm 0.03$	0.97 ± 0.02
Γ_s $[\mathrm{ps}^{-1}]$	$+0.680 \pm 0.003$	$+0.08 \pm 0.03$	1.04 ± 0.02
$\Delta\Gamma_\mathrm{s}$ $[\mathrm{ps}^{-1}]$	$+0.050 \pm 0.009$	$+0.10 \pm 0.03$	0.96 ± 0.02
$\phi_\mathrm{s}^{\mathrm{J}/\psi\phi}$	-0.609 ± 0.200	-0.04 ± 0.03	1.04 ± 0.02
$\delta_{\lvert\rvert}$ [rad]	-2.926 ± 0.064	$+0.10 \pm 0.03$	1.09 ± 0.02
$\delta_\perp$ [rad]	$+2.910 \pm 0.177$	$+0.00 \pm 0.03$	0.99 ± 0.02

Table 12 Sensitivities and pull distribution parameters obtained with 2 fb^{-1} of Toy Monte Carlo data.

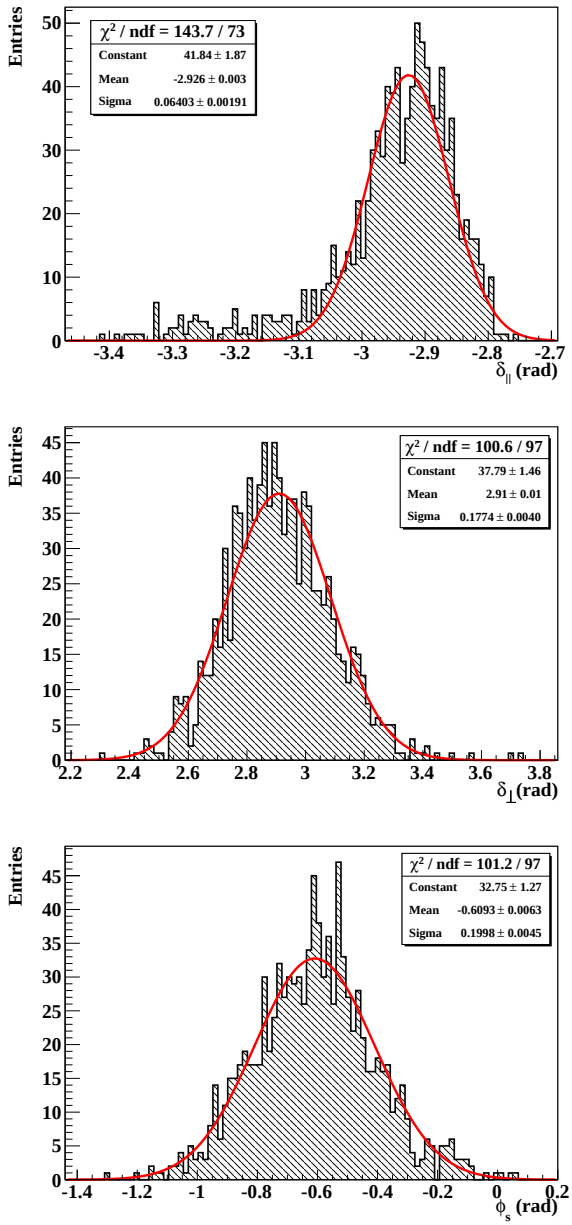

Figure 6 $\delta_{||}$ (top), $\delta_\perp$ (middle) and $\phi_\mathrm{s}^{\mathrm{J}/\psi\phi}$ (bottom) output fit value distributions obtained for 2 fb^{-1} of toy Monte Carlo data, with strong phases Gaussian-constrained with $\sigma = 0.18$ rad.

The sensitivities to the $|A_0|^2$, $|A_\perp|^2$, Γ_s and $\Delta\Gamma_\mathrm{s}$ parameters are found to be ± 0.003, ± 0.004, ± 0.003 ps^{-1} and ± 0.009 ps^{-1} respectively, which are similar to the ones of Table 8.

The sensitivity to $\delta_\perp$ is equal to $\sigma_{\mathrm{meas}} = 0.18$ rad, which means that it is fully dominated by the external constraint, whereas the sensitivity to $\delta_{||}$ of ± 0.06 rad is dominated by the parameter determination with data, as being smaller than σ_{meas}.

The sensitivity to $\phi_\mathrm{s}^{\mathrm{J}/\psi\phi}$ is ± 0.20 rad for 2 fb^{-1} of data at $\sqrt{s} = 14$ TeV[1].

6 Conclusions

The measurement of the CP violating phase $\phi_\mathrm{s}^{\mathrm{J}/\psi\phi}$ is one of the most important measurements that will be performed at LHCb. In the Standard Model, this phase is predicted to be $\phi_\mathrm{s}^{\mathrm{J}/\psi\phi} = -0.0360^{+0.0020}_{-0.0016}$ rad, which makes it one of the CP observables with the smallest theoretical uncertainty. New physics contributions could significantly modify this prediction. With early data, a simplified time-dependent angular analysis can be performed, which does not require the flavor of the $\mathrm{B_s^0}$ meson at production to be known. Studies presented in this document show that with 2 fb^{-1} of data at $\sqrt{s} = 14$ TeV, a sensitivity to $\phi_\mathrm{s}^{\mathrm{J}/\psi\phi}$ of ± 0.20 rad is expected, in the case of a New Physics scenario, i.e. large CP violation effect ($\phi_\mathrm{s}^{\mathrm{J}/\psi\phi} \sim 0.60$ rad). If the phase is small as expected by the Standard model, others parameters can be measured, such as the amplitudes of the CP-even and CP-odd components, ($|A_0|^2 + |A_{||}|^2$) and $|A_\perp|^2$, the $\mathrm{B_s^0}$ meson lifetime $\tau_s = 1/\Gamma_\mathrm{s}$, and the width difference $\Delta\Gamma_\mathrm{s}$ between the two mass eigenstates. With only 0.2 fb^{-1} of data at $\sqrt{s} = 14$ TeV, these measurements would become more precise statistically than the latest results quoted by the CDF experiment (June 2010).

7 References

[1] The LHCb Collaboration, *Road map for the selected key measurements of LHCb*, CERN Report LHCb-PUB-2009-029.

[2] The β_s working group, *Sensitivity Studies (v2)*, https://twiki.cern.ch/twiki/bin/view/LHCb/ParamSensit

[3] M. Calvi et al., *Lifetime unbiased selection of* $\mathrm{B_s^0} \to \mathrm{J/\psi\phi}$ *and related control channels :* $\mathrm{B^0} \to \mathrm{J/\psi K^{*0}}$ *and* $\mathrm{B^+} \to \mathrm{J/\psi K^+}$, CERN Report LHCb-2009-025.

[4] P. Vankov et al., *Proper time resolution modelling*, CERN Report LHCb-2007-055.

[5] G. Conti and A. Hicheur, *Angular Acceptance Parameterization for* $\mathrm{B_s^0} \to \mathrm{J/\psi\phi}$ *Studies*, CERN Report LHCb-INT-2010-046.

[6] P. Clarke et al., *Sensitivity studies to* β_s *and* $\Delta\Gamma_s$ *using the full* $\mathrm{B_s^0} \to \mathrm{J/\psi\phi}$ *angular analysis at the LHCb*, CERN Report LHCb-2007-101.

[7] The β_s working group, *Software data*, https://twiki.cern.ch/twiki/bin/view/LHCb/BetasCodeVersions

[8] T. d Pree et al., *Methods for angular analyses of* $B \to J/\psi V$, CERN Report LHCb-2009-024.

[9] W. Verkerke et al., *The RooFit Toolkit for data modeling*, Proceeding to PHYSTAT05, http://roofit.sourceforge.net

[10] F. James, *Minuit, Function Minimization and Error Analysis*, CERN long writeup D506.

[11] C. Langenbruch et al., *Fit of the decay* $\mathrm{B_s^0} \to \mathrm{J/\psi\phi}$, CERN Report LHCb-2009-028.

[12] M. Williams, *CP Violation Measurements At The Tevatron*, FERMILAB-CONF-10-231-E (EW Moriond 2010).

[1] No sensitivity studies are performed for the 0.2 and 0.1 fb^{-1} of data. Biases in $\Delta\Gamma_s$ and underestimations of the errors for $\phi_\mathrm{s}^{\mathrm{J}/\psi\phi}$ have been observed for these statistical scenarios, in the case the strong phases were fixed (Appendix 8.2). Similar observations are hence expected for the case discussed here in which the strong phases are Gaussian-constrained.

[13] The CDF/D⊘ $\Delta\Gamma_s$, β_s Combination Working Group, *Combination of D⊘ and CDF Results on* $\Delta\Gamma_s$ *and the CP-Violating Phase* $\beta_s^{J\psi\phi}$, CDF/PHYS/BOTTOM/CDFR/9787, D⊘ Note 5928-CONF.

[14] The CDF Collaboration, *An Updated Measurement of the CP Violating Phase* $\beta_s^{J/\psi\phi}$ *in* $\mathrm{B_s^0} \to \mathrm{J/\psi\phi}$ *Decays using 5.2* fb^{-1} *of Integrated Luminosity*, CDF/ANAL/BOTTOM/PUBLIC/10206.

[15] C. Amsler et al. (Particle Data Group), *The CKM Quark-Mixing Matrix*, Phys. Rev. Lett. B 667, 1 (2008).

[16] The Babar Collaboration, *Measurement of decay amplitudes of* $B \to J/\psi\ K^*$, $\psi(2S)\ K^*$, *and* $\chi_{c1}\ K^*$ *with an angular analysis*, Phys. Rev. D-RC 76, 031102 (2007).

[17] M. Gronau et al., *Flavor symmetry for strong phases and determination of* β_s, $\Delta\Gamma$ *in* $\mathrm{B_s^0} \to \mathrm{J/\psi\phi}$, [arXiv:0808.3761].

[18] The D⊘ Collaboration, *Measurement of* B_s^0 *mixing parameters from the flavor-tagged decay* $\mathrm{B_s^0} \to \mathrm{J/\psi\phi}$, Phys. Rev. Lett. 101, 241801 (2008).

[19] J. Charles et al. (CKMfitter group), *CP Violation and the CKM Matrix: Assessing the Impact of the Asymmetric B Factories*, Eur. Phys. J. C41, 1-131 (2005), [hep-ph/ 0406184v3], updated results and plots available at http://ckmfitter.in2p3.fr/

8 Appendix

8.1 Fixing the Strong and Weak Phases

In this scenario, the $\delta_{||}$ and $\delta_{\perp}$ strong phases are fixed to their input values and $\phi_{\mathrm{s}}^{\mathrm{J}/\psi\phi}$ is fixed to its Standard Model prediction (Table 7). Only four physics parameters remain free in the fit, $|A_0|^2$, $|A_{\perp}|^2$, Γ_{s} and $\Delta\Gamma_{\mathrm{s}}$. This scenario is an update of the previous work performed at LHCb on the fit to untagged $\mathrm{B_s^0} \to \mathrm{J/\psi\phi}$ events [6]. Results are added for the 0.2 and 0.1 fb^{-1} statistical scenarios.

Results for $2\ \mathrm{fb}^{-1}$ of data are shown in the upper part of Table 13 using the P2VV fitter. They give sensitivities of ± 0.003 for $|A_0|^2$, ± 0.004 for $|A_{\perp}|^2$, $\pm 0.003\ \mathrm{ps}^{-1}$ for Γ_{s} and $\pm 0.008\ \mathrm{ps}^{-1}$ for $\Delta\Gamma_{\mathrm{s}}$. No biases are observed in the pull distributions.

The results are validated using the Heidelberg fitter (Table 13). Adding the angular acceptance variation parameterization [5] to the fit model used in P2VV fitter does not induce any significant changes. A comparison is also made with fixing in the fit model $\phi_{\mathrm{s}}^{\mathrm{J}/\psi\phi}$ to its New Physics value (Table 7) instead. Similar parameter sensitivities are observed (Table 13).

Parameters	Value and Sensitivity	Pull Mean	Pull Width
Result With P2VV Fitter			
$\lvert A_0\rvert^2$	0.556 ± 0.003	$+0.01 \pm 0.06$	1.01 ± 0.04
$\lvert A_{\perp}\rvert^2$	0.233 ± 0.004	$+0.06 \pm 0.06$	0.99 ± 0.04
$\Gamma_{\mathrm{s}}\ [\mathrm{ps}^{-1}]$	0.680 ± 0.003	$+0.04 \pm 0.06$	0.96 ± 0.04
$\Delta\Gamma_{\mathrm{s}}\ [\mathrm{ps}^{-1}]$	0.049 ± 0.008	-0.01 ± 0.06	1.00 ± 0.04
Comparison With Heidelberg Fitter			
$\lvert A_0\rvert^2$	0.556 ± 0.003	$+0.06 \pm 0.06$	1.00 ± 0.04
$\lvert A_{\perp}\rvert^2$	0.233 ± 0.004	-0.06 ± 0.06	0.94 ± 0.04
$\Gamma_{\mathrm{s}}\ [\mathrm{ps}^{-1}]$	0.680 ± 0.003	-0.06 ± 0.06	1.02 ± 0.04
$\Delta\Gamma_{\mathrm{s}}\ [\mathrm{ps}^{-1}]$	0.049 ± 0.008	$+0.05 \pm 0.06$	0.95 ± 0.04
Including Angular Acceptances (P2VV Fitter)			
$\lvert A_0\rvert^2$	0.556 ± 0.003	-0.08 ± 0.06	0.96 ± 0.04
$\lvert A_{\perp}\rvert^2$	0.233 ± 0.003	$+0.06 \pm 0.06$	0.98 ± 0.04
$\Gamma_{\mathrm{s}}\ [\mathrm{ps}^{-1}]$	0.680 ± 0.003	$+0.01 \pm 0.06$	0.98 ± 0.04
$\Delta\Gamma_{\mathrm{s}}\ [\mathrm{ps}^{-1}]$	0.049 ± 0.008	-0.02 ± 0.06	0.95 ± 0.04
With New Physics Scenario (P2VV Fitter)			
$\lvert A_0\rvert^2$	0.556 ± 0.002	$+0.03 \pm 0.06$	0.99 ± 0.04
$\lvert A_{\perp}\rvert^2$	0.233 ± 0.003	$+0.00 \pm 0.06$	1.02 ± 0.04
$\Gamma_{\mathrm{s}}\ [\mathrm{ps}^{-1}]$	0.680 ± 0.002	$+0.03 \pm 0.06$	1.02 ± 0.04
$\Delta\Gamma_{\mathrm{s}}\ [\mathrm{ps}^{-1}]$	0.049 ± 0.008	-0.02 ± 0.06	1.03 ± 0.04

Table 13 Sensitivities and pull distribution parameters for 2 fb^{-1} of toy Monte Carlo data.

Results with lower statistics are given in Tables 14 and 15 for $0.2\ \mathrm{fb}^{-1}$ and $0.1\ \mathrm{fb}^{-1}$ respectively. In both cases, the results are comparable for the four different cases studied. The sensitivities scale as $\sqrt{N}$, with N the number of $\mathrm{B_s^0} \to \mathrm{J/\psi\phi}$ events: ± 0.009 for $|A_0|^2$ and Γ_{s}, ± 0.011 for $|A_{\perp}|^2$ and ± 0.026 for $\Delta\Gamma_{\mathrm{s}}$ with 0.2 fb^{-1}, ± 0.012 for $|A_0|^2$ and Γ_{s}, ± 0.016 for $|A_{\perp}|^2$ and ± 0.038 for $\Delta\Gamma_{\mathrm{s}}$ with 0.1 fb^{-1}.

No biases are observed in the pull distributions for both cases. This means that with only $0.1\ \mathrm{fb}^{-1}$ of real data, the four parameters can already be determined with some sensitivity without encountering stability problems from the minimization procedure.

Parameters	Value and Sensitivity	Pull Mean	Pull Width
Result With P2VV Fitter			
$\lvert A_0\rvert^2$	0.556 ± 0.009	-0.05 ± 0.06	1.04 ± 0.04
$\lvert A_\perp\rvert^2$	0.234 ± 0.011	$+0.05 \pm 0.06$	1.03 ± 0.04
Γ_s $[\mathrm{ps}^{-1}]$	0.680 ± 0.009	-0.01 ± 0.06	0.98 ± 0.04
$\Delta\Gamma_\mathrm{s}$ $[\mathrm{ps}^{-1}]$	0.048 ± 0.025	-0.03 ± 0.06	0.99 ± 0.04
Comparison With Heidelberg Fitter			
$\lvert A_0\rvert^2$	0.556 ± 0.009	$+0.02 \pm 0.06$	0.96 ± 0.04
$\lvert A_\perp\rvert^2$	0.234 ± 0.012	$+0.03 \pm 0.06$	0.94 ± 0.04
Γ_s $[\mathrm{ps}^{-1}]$	0.681 ± 0.009	$+0.06 \pm 0.06$	0.98 ± 0.04
$\Delta\Gamma_\mathrm{s}$ $[\mathrm{ps}^{-1}]$	0.048 ± 0.027	-0.01 ± 0.06	0.93 ± 0.04
Including Angular Acceptances (P2VV Fitter)			
$\lvert A_0\rvert^2$	0.556 ± 0.008	$+0.00 \pm 0.06$	1.00 ± 0.04
$\lvert A_\perp\rvert^2$	0.233 ± 0.011	$+0.02 \pm 0.06$	1.01 ± 0.04
Γ_s $[\mathrm{ps}^{-1}]$	0.680 ± 0.009	-0.02 ± 0.06	1.00 ± 0.04
$\Delta\Gamma_\mathrm{s}$ $[\mathrm{ps}^{-1}]$	0.049 ± 0.026	$+0.06 \pm 0.06$	1.05 ± 0.04
With New Physics Scenario (P2VV Fitter)			
$\lvert A_0\rvert^2$	0.556 ± 0.008	-0.04 ± 0.06	1.06 ± 0.04
$\lvert A_\perp\rvert^2$	0.234 ± 0.011	$+0.03 \pm 0.06$	1.04 ± 0.04
Γ_s $[\mathrm{ps}^{-1}]$	0.680 ± 0.008	-0.04 ± 0.06	1.05 ± 0.04
$\Delta\Gamma_\mathrm{s}$ $[\mathrm{ps}^{-1}]$	0.049 ± 0.027	$+0.03 \pm 0.06$	1.07 ± 0.04

Table 14 Sensitivities and pull distribution parameters for 0.2 fb^{-1} of toy Monte Carlo data.

Parameters	Value and Sensitivity	Pull Mean	Pull Width
Result With P2VV Fitter			
$\lvert A_0\rvert^2$	0.555 ± 0.012	-0.08 ± 0.06	1.09 ± 0.04
$\lvert A_\perp\rvert^2$	0.235 ± 0.016	$+0.08 \pm 0.06$	1.05 ± 0.04
Γ_s $[\mathrm{ps}^{-1}]$	0.681 ± 0.012	$+0.06 \pm 0.06$	0.98 ± 0.04
$\Delta\Gamma_\mathrm{s}$ $[\mathrm{ps}^{-1}]$	0.045 ± 0.037	-0.07 ± 0.06	1.03 ± 0.04
Comparison With Heidelberg Fitter			
$\lvert A_0\rvert^2$	0.557 ± 0.013	$+0.06 \pm 0.06$	0.96 ± 0.04
$\lvert A_\perp\rvert^2$	0.234 ± 0.019	$+0.01 \pm 0.06$	1.03 ± 0.04
Γ_s $[\mathrm{ps}^{-1}]$	0.682 ± 0.013	$+0.08 \pm 0.06$	0.98 ± 0.04
$\Delta\Gamma_\mathrm{s}$ $[\mathrm{ps}^{-1}]$	0.049 ± 0.039	$+0.04 \pm 0.06$	0.99 ± 0.04
Including Angular Acceptances (P2VV Fitter)			
$\lvert A_0\rvert^2$	0.555 ± 0.011	-0.05 ± 0.06	0.94 ± 0.04
$\lvert A_\perp\rvert^2$	0.234 ± 0.016	$+0.03 \pm 0.06$	1.05 ± 0.04
Γ_s $[\mathrm{ps}^{-1}]$	0.681 ± 0.012	$+0.06 \pm 0.06$	1.00 ± 0.04
$\Delta\Gamma_\mathrm{s}$ $[\mathrm{ps}^{-1}]$	0.046 ± 0.036	-0.04 ± 0.06	0.97 ± 0.04
With New Physics Scenario (P2VV Fitter)			
$\lvert A_0\rvert^2$	0.556 ± 0.012	-0.01 ± 0.06	1.15 ± 0.05
$\lvert A_\perp\rvert^2$	0.234 ± 0.014	$+0.02 \pm 0.06$	1.00 ± 0.04
Γ_s $[\mathrm{ps}^{-1}]$	0.681 ± 0.011	$+0.06 \pm 0.06$	0.99 ± 0.04
$\Delta\Gamma_\mathrm{s}$ $[\mathrm{ps}^{-1}]$	0.045 ± 0.037	-0.07 ± 0.06	1.02 ± 0.04

Table 15 Sensitivities and pull distribution parameters for 0.1 fb^{-1} of toy Monte Carlo data.

8.2 New Physics Scenario with Fixing the Strong Phases

A possibility to solve the problem in the determination of the $\delta_{||}$ and $\delta_{\perp}$ strong phases would be to fix them. This solution is not optimal, as it requires an external knowledge. The $\delta_{||}$ and $\delta_{\perp}$ strong phases measured by the Babar collaboration in the $\mathrm{B^0} \to \mathrm{J/\psi K^{*0}}$ channel [16] would be used, as they should be similar to the ones of the $\mathrm{B_s^0} \to \mathrm{J/\psi\phi}$ channel under flavor symmetry. This assumption seems reasonable, as they are expected to be equal within a similar precision of a few percent of π (or $\sim 10°$) [17].

Sensitivity results are given in Table 16 for 2 $\mathrm{fb^{-1}}$ of data. The sensitivity to $\phi_\mathrm{s}^{\mathrm{J}/\psi\phi}$ is ± 0.19 rad.

Parameters	Value and Sensitivity	Pull Mean	Pull Width
Results With P2VV Fitter			
$\lvert A_0\rvert^2$	0.556 ± 0.003	-0.05 ± 0.06	1.01 ± 0.04
$\lvert A_\perp\rvert^2$	0.233 ± 0.003	$+0.06 \pm 0.06$	0.98 ± 0.04
Γ_s $[\mathrm{ps^{-1}}]$	0.680 ± 0.003	$+0.10 \pm 0.06$	1.03 ± 0.04
$\Delta\Gamma_\mathrm{s}$ $[\mathrm{ps^{-1}}]$	0.049 ± 0.008	$+0.04 \pm 0.06$	1.02 ± 0.04
$\phi_\mathrm{s}^{\mathrm{J}/\psi\phi}$ [rad]	-0.610 ± 0.181	-0.07 ± 0.06	0.99 ± 0.04
Validation With Heidelberg Fitter			
$\lvert A_0\rvert^2$	0.556 ± 0.003	$+0.06 \pm 0.06$	1.02 ± 0.04
$\lvert A_\perp\rvert^2$	0.233 ± 0.004	-0.06 ± 0.06	0.95 ± 0.04
Γ_s $[\mathrm{ps^{-1}}]$	0.680 ± 0.003	-0.04 ± 0.06	1.03 ± 0.04
$\Delta\Gamma_\mathrm{s}$ $[\mathrm{ps^{-1}}]$	0.050 ± 0.009	$+0.12 \pm 0.06$	0.94 ± 0.04
$\phi_\mathrm{s}^{\mathrm{J}/\psi\phi}$ [rad]	-0.589 ± 0.188	$+0.06 \pm 0.06$	1.03 ± 0.04

Table 16 Sensitivities and pull distribution parameters obtained for 2 $\mathrm{fb^{-1}}$ of Toy Monte Carlo data.

Sensitivity results are given in Table 17 for 0.2 $\mathrm{fb^{-1}}$ of Toy Monte Carlo data. No sensitivity to $\phi_\mathrm{s}^{\mathrm{J}/\psi\phi}$ is left. A bias in the $\Delta\Gamma_\mathrm{s}$ pull distribution is observed and the errors are underestimated for $\phi_\mathrm{s}^{\mathrm{J}/\psi\phi}$, as the pull distribution widths equal ~ 1.2 (Table 17) (highlighted in yellow).

Parameters	Value and Sensitivity	Pull Mean	Pull Width
Result With P2VV Fitter			
$\lvert A_0\rvert^2$	0.556 ± 0.008	$+0.03 \pm 0.06$	0.98 ± 0.04
$\lvert A_\perp\rvert^2$	0.232 ± 0.011	-0.07 ± 0.06	1.00 ± 0.04
Γ_s $[\mathrm{ps^{-1}}]$	0.681 ± 0.009	$+0.04 \pm 0.06$	1.01 ± 0.04
$\Delta\Gamma_\mathrm{s}$ $[\mathrm{ps^{-1}}]$	$+0.060 \pm 0.026$	$+0.41 \pm 0.06$	0.97 ± 0.04
$\phi_\mathrm{s}^{\mathrm{J}/\psi\phi}$ [rad]	-0.567 ± 0.566	-0.02 ± 0.06	1.19 ± 0.04
Validation With Heidelberg Fitter			
$\lvert A_0\rvert^2$	0.556 ± 0.009	$+0.03 \pm 0.06$	0.94 ± 0.04
$\lvert A_\perp\rvert^2$	0.234 ± 0.013	$+0.04 \pm 0.06$	0.93 ± 0.04
Γ_s $[\mathrm{ps^{-1}}]$	0.682 ± 0.010	$+0.15 \pm 0.06$	0.97 ± 0.04
$\Delta\Gamma_\mathrm{s}$ $[\mathrm{ps^{-1}}]$	0.057 ± 0.029	$+0.29 \pm 0.06$	0.91 ± 0.04
$\phi_\mathrm{s}^{\mathrm{J}/\psi\phi}$ [rad]	-0.570 ± 0.647	$+0.04 \pm 0.06$	1.22 ± 0.04

Table 17 Sensitivities and pull distribution parameters obtained with 0.2 $\mathrm{fb^{-1}}$ of Toy Monte Carlo data (biases highlighted in yellow).